Iranian Journal of Oil & Gas Science and Technology, Vol. 2 (2013), No. 2, pp. 50-64
http://ijogst.put.ac.ir

CFD Simulation of Dimethyl Ether Synthesis from Methanol in an Adiabatic Fixed-bed Reactor

M. Golshadi[1], R. Mosayebi Behbahani[1*], and M. Irani[2]

[1] Department of Gas Engineering, Petroleum University of Technology, Ahwaz, Iran
[2] Research Institute of Petroleum Industry (RIPI), Tehran, Iran

Abstract

A computational fluid dynamic (CFD) study of methanol (MeOH) to dimethyl ether (DME) process in an adiabatic fixed-bed reactor is presented. One of the methods of industrial DME production is the catalytic dehydration of MeOH. Kinetic model was derived based on Bercic rate. The parameters of this equation for a specific catalyst were tuned by solving a one-dimensional homogenous model using MATLAB optimization module. A two-dimensional CFD simulation of the reaction is demonstrated and considered as numerical experiments. A sensitivity analysis was run in order to find the effect of temperature, pressure, and WHSV on the reactor performance. Good agreement was achieved between bench experimental data and the model. The results show that the maximum conversion of reaction (about 85.03%) is obtained at WHSV=10 h^{-1} and T=563.15 K, whereas the inlet temperature has a greater effect on methanol conversion. Moreover, the effect of water in inlet feed on methanol conversion is quantitatively studied. It was concluded that the results obtained from CFD analysis give precise guidelines for further studies on the optimization of reactor performance.

Keywords: CFD, DME, Methanol Dehydration, Adiabatic, Fixed-bed Reactor

1. Introduction

Nowadays, environmental impacts of greenhouse gas pollutants emitted from the combustion of fossil fuels on the one hand, and legal regulations against the production of air pollutants (Euro IV) on the other hand, have constantly increased the necessity of using clean fuels. Although the use of green energy such as solar and geothermal energies might be the ultimate goal for this, the development of synthetic energy is a currently high priority task. Among synthetic energy resources, DME is one of the most promising energy resources because it has better environmental performance as well as properties similar to traditional fuels (Yoon and C. Han, 2009). DME is the simplest ether, with a chemical formula of CH_3OCH_3. It is a volatile organic compound, but non-teratogenic, non-mutagenic, and non-toxic (Olah et al., 2009); it has a boiling point of -25 °C and a vapor pressure of about 0.6 MPa at ambient temperature, which makes it easily liquefied. DME can be synthesized from natural gas, coal, biomass, and/or coal seam, and is a sulfur-free, near-zero aromatic synthetic fuel which is considered an excellent substitute for conventional diesel and liquefied petroleum gas (LPG) (Yoon and C. Han, 2009) and has a considerable potential in power generation for medium-sized power plants especially on islands (Semelsberger et al., 2006). It has also been used to produce dimethyl sulfate (Cheung et al., 2006) and light olefins (Ivanova et al., 2009).

[*] Corresponding Author:
Email: behbahani@put.ac.ir

The aforementioned applications and descriptions made DME as a future clean fuel of the 21st century. It has been reported that using syngas (CO,H_2) as a starting material, DME can be prepared in a one-step process in which all steps are exothermic reactions, and thereby making the overall reaction a highly exothermic process (Lu et al,. 2004). Alcohols dehydration reaction is another important route to produce ethers (Ivanova et al., 2009). In this method which is named indirect process, methanol is converted to DME in a catalytic dehydration reactor over a solid-acid catalyst by the following reaction (Raoof et al., 2008):

$$2CH_3OH \leftrightarrow CH_3OCH_3 + H_2O \qquad \Delta H = -21.255 \text{ kj/mol} \tag{1}$$

The dehydration of methanol is in gas phase and a moderate exothermic reaction. The heat of reaction is considerably small in comparison with the one-step process. Currently, this method is known and proven completely in large scale plants; hence DME is manufactured commercially by this process in the adiabatic fixed-bed reactor in the temperature range of 200 °C to 400 °C and at pressures up to 2 Mpa over solid acid catalysts such as γ-Al_2O_3 and molecular sieve materials (such as zeolites, chabazites, SAPOs, etc.) (Khom-in et al., 2008). A review on the catalyst of the reaction is presented by Spivey (Spivey 1991). Many researchers have investigated the reaction on different catalysts (Fazlollahnejad et al., 2009; Raoof et al., 2008; Hosseini and Khosravi Nikou, 2012; Cheung et al., 2006). Another way to attain a better uptake of the reaction is modeling and optimizing; some researchers have worked on this way (Bercic and Levec, 1993; Farsi et al., 2010; Lu et al., 2004).
In the design of fixed-bed reactors, fluid dynamics plays an important role since the transport of the chemical species and mixing are entirely described by the conservation laws. CFD is the field of solving these complex non-linear differential equations governing fluid flow using numerical methods. Two approaches are considered in CFD for modeling fixed-bed reactors, namely one pseudo continuum approach, in which both fluid and solid phases are modeled as interpenetrating continua (Figure 1.a); an example of this approach is Shahhosseini's work (Shahhosseini et al., 2009).

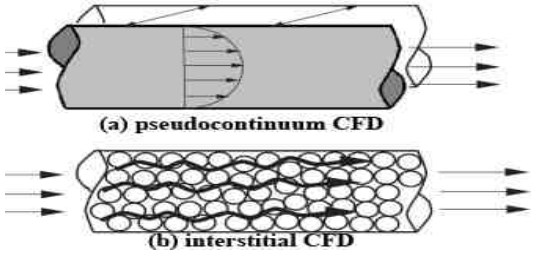

Figure 1
Comparison of (a) pseudo-continuum and (b) interstitial CFD approaches to packed tube simulation (Andrews et al., 2006).

An alternative and complementary use of CFD in fixed-bed simulation has been to solve the actual flow field between the particles (Figure 1.b). This approach does not simplify the geometrical complexities of the packing and thus geometry configuration must exactly be known. An example of fixed bed modeling in this way is given elsewhere (Freund et al., 2003). In the present study, methanol dehydration reaction simulation in a fixed-bed bench-scale reactor is investigated and the pseudo continuum CFD approach is used. For the validation of the simulation results we used the pervious experimental data of the work done in the same reactor set in the institute (Ghavipour, 2011) Catalyst characteristics and some important results of this work have been listed in Table 1.

Table 1
Catalyst characteristics and important results of (Ghavipour 2011) work.

Catalyst characterizations (γ-Alumina from Engelhard Corporation)					
Particle size distribution		Bulk density(g/cm^3)		BET surface area (m^2/g$_{cat.}$)	
%98 di$_p$>0.06mm, %4 d_p>0.2 mm		0.896		183.206	
Reactor diameter size(d_t)=3/8 inch, catalyst amount= 1.05 gr, WHSV=90 gr$_{MeOH}$/gr$_{cat.}$h					
T(°C)	250	275	300	325	350
Methanol conversion	0.0793	0.2295	0.4741	0.7268	0.816

2. Theoretical background

Based on (Dybbs and Edwards, 1984) criterion, the flow regime in these experiments is laminar flow. Laminar flow through circular ducts requires a two-dimensional flow model to describe the velocity and concentration field accurately in both radial and axial direction (Schuurman, 2008). The dispersion model in this work cannot be used because of following reasons: firstly d_p/d_{tube}<0.1 and secondly L_{tube}/d_{tube}<50 according to Fazlollahnejad's study (Fazlollahnejad et al., 2009). On the other hand, if an exothermic reaction occurring in an adiabatic bed is associated with a mild heat generation, pseudo-homogeneous models are suitable to describe the behavior of the reactor (Andrigo et al., 1999). Also, the interfacial and inter-particle resistance of mass and heat transfer in catalyst particles can be omitted. Therefore, a pseudo-continuum plug-flow two-dimensional homogeneous reaction model is chosen to simulate the steady state adiabatic fixed-bed reactor and an axially symmetric model is employed into FLUENT. Thus the continuity, momentum, energy, and species transport equations are in the forms of:

$$\frac{\partial}{\partial z}(\rho v_z) + \frac{\partial}{\partial r}(\varepsilon\, \rho v_r) + \frac{\varepsilon\, \rho v_r}{r} = 0 \tag{2}$$

$$\frac{1}{r}\frac{\partial}{\partial z}(\varepsilon r \rho v_z v_z) + \frac{1}{r}\frac{\partial}{\partial r}(\varepsilon r \rho v_r v_z) = -\varepsilon\frac{\partial P}{\partial z} + \frac{2}{r}\frac{\partial}{\partial z}\left[\varepsilon r \mu \frac{\partial v_z}{\partial z}\right] + \frac{1}{r}\frac{\partial}{\partial r}\left[\varepsilon r \mu \left(\frac{\partial v_z}{\partial r} + \frac{\partial v_r}{\partial z}\right)\right] + F_z$$

$$\frac{1}{r}\frac{\partial}{\partial z}(\varepsilon r \rho v_z v_r) + \frac{1}{r}\frac{\partial}{\partial r}(\varepsilon r \rho v_r v_r) = -\varepsilon\frac{\partial P}{\partial r} + \frac{2}{r}\frac{\partial}{\partial r}\left[\varepsilon r \mu \frac{\partial v_r}{\partial r}\right] + \frac{1}{r}\frac{\partial}{\partial z}\left[\varepsilon r \mu \left(\frac{\partial v_z}{\partial r} + \frac{\partial v_r}{\partial z}\right)\right] - 2\varepsilon\mu\frac{v_r}{r^2} + F_r \tag{3}$$

$$v.\rho\, c_{pf}\frac{\partial T}{\partial z} - \frac{\lambda_{er}}{r}\frac{\partial}{\partial r}\left(r\frac{\partial T}{\partial r}\right) = \rho_b \sum_i (-\Delta H_i).\hat{r}_i(C,T) \tag{4}$$

$$v.\frac{dC_j}{dZ} - \frac{\varepsilon.D_{ejm}}{r}\frac{\partial}{\partial r}\left(r\frac{\partial C_j}{\partial r}\right) = \rho_b.R_j(C,T) \tag{5}$$

where, z and r are the axial and radial coordinates; v is velocity vector; P and T stand for the static pressure and temperature respectively; ρ_b and C_j represents bulk density of bed and the concentration of chemical species; ΔH_i is the heat of reaction I; $\hat{r}_i(C,T)$ represents the rate of ith reaction; $R_j = \sum_{i=1}^{NR} \alpha_{ij}.\hat{r}_i$ is the rate of production of species j; α_{ij} represents stoichiometric coefficient for species j in ith reaction. It is assumed that the reactor bed is a porous zone with extra terms in the momentum balance equation (F_i in equation 3) to allow for additional resistance against flow, which can be modeled in the form of Ergun's equation (Ergun, 1952):

$$F_i = -\left(\sum_{j=1}^{2} A_{ij}\mu v_j + \sum_{j=1}^{2} B_{ij}\frac{1}{2}\rho|v|v_j\right) \tag{6}$$

where, according to Ergun's equation: $A=\frac{150}{d_P^2}\frac{(1-\varepsilon)^2}{\varepsilon^3}$, $B=\frac{3.5}{d_P}\frac{(1-\varepsilon)}{\varepsilon^3}$; ρ stands for mixture density and is determined by ideal gas law due to atmospheric pressure; ε is bed voidage and is calculated from the correlation given by Anthony G Dixon (Anthony G Dixon, 1988):

$$\text{For spheres, } \varepsilon = \begin{cases} 0.4 + 0.05\left(d_p/d_t\right) + 0.412\left(d_p/d_t\right)^2, d_p/d_t \le 0.5 \\ 0.528 + 2.464\left(d_p/d_t - 0.5\right), 0.5 \le d_p/d_t \le 0.536 \\ 1 - 0.667\left(d_p/d_t\right)^3\left(2\,d_p/d_t - 1\right)^{-0.5}, d_p/d_t \ge 0.536 \end{cases} \quad (7)$$

The average particle diameter (d_p) for granular solids of mixed sizes may be calculated as given elsewhere (Tilton and Hottel, 2008):

$$\frac{1}{d_P} = \sum_i \frac{m_i}{d_{P,i}} \quad (8)$$

where, m_i is the weight fraction of particles of size $d_{P,i}$. In the above equations, for specific heat capacity (C_{pf}), viscosity (μ), and conductivity (λ_{er}) of the mixture, user-defined function (UDF) codes are written and inserted into FLUENT cases. The codes are constructed based on mixing laws and Perry's handbook correlations of species individual properties (Tilton and Hottel et al., 2008) as summarized in Tables 2 and 3.

Table 2
Correlation for individual C_p

C_P (J/Kg.K) = $a + bT + cT^2 + dT^3 + eT^4$					
Constants	*a*	*b*	*C*	*d*	*e*
Water	1914.5	-0.79148	2.6286e-3	1.98022e-6	5.1923e-10
DME	369.68	3.8902	1.1369e-3	-4.16588e-8	-
MeOH	660.2	2.2144	8.0777e-4	-9.0424e-7	-

Table 3
Individual viscosity and conductivity correlations

Corr.	$\mu = \frac{C_1 T^{C_2}}{1 + C_3/T + C_4/T^4}$					$\lambda = \frac{C_1 T^{C_2}}{1 + C_3/T + C_4/T^2}$				
constants	C_1	C_2	C_3	C_4	Temp. Range(K)	C_1	C_2	C_3	C_4	Temp. Range(K)
Water	1.7e-6	1.114	-	-	273 – 1073	6.2e-6	1.397	-	-	273 – 1073
DME	2.6e-6	0.397	534	-	131 – 1000	0.059	0.266	1018.6	1098800	248 – 1500
MeOH	3.0e-7	0.696	205	-	240 – 1000	5.7e-7	1.786	-	-	273 – 684

One parameter for the identification between Knudsen or bulk diffusion in porous zones is $\ell(m) = \frac{3.2\mu}{P}\left(\frac{RT}{2\pi M}\right)^{1/2}$ (ℓ= mean free path of the gas molecule, M=molecular weight, R= universal gas constant). In according to Perry's handbook, when $\frac{\ell}{\text{pore diameter of paricle(m)}} < 0.01$ (similar to our case), the bulk diffusion is the more important part of the diffusion and $D_{ejm} = \frac{\varepsilon D_{jm}}{\tau_o}$. For the estimation of the tortuosity (τ_o) of bed, a more recent correlation that is presented by Lanfrey (Lanfrey et al., 2010) is used:

$\tau_o = 1.23\frac{(1-\varepsilon)^{4/3}}{\varepsilon\phi^2}$, ($\phi$ is particles sphericity factor) (9)

Klusacek (Klusacek and Schneider, 1981) claimed that the bulk diffusion of the multicomponent mixture (D_{jm}) in this reaction on a porous catalyst can be satisfactorily described by Stefan-Maxwell equations. Therefore, we turned on the FULLCOMPONENT diffusion in FLUENT and the binary diffusivity (D_{jk}) in this equation is described by the correlation of (Brokaw, 1969), which is suitable for polar mixtures.

2.1. Reaction rate model

The kinetic of methanol dehydration on acidic catalysts has extensively been studied. In this study, a summary of the published kinetic models from different works (Bercic and Levec, 1992; Mollavali et al., 2008; Moradi et al., 2010; L. Zhang et al., 2011 Padmanabhan and Eastburn, 1972) is given in Table 4. Many researchers have used Bercic's rate equation in their works and this equation is more global than other proposed equations (Fazlollahnejad et al., 2009; Farsi et al., 2010; Moradi et al., 2010; Mollavali et al., 2008).

2.2. Equilibrium constant

There are few studies to determine equilibrium constant of the reaction. A study about equilibrium constant is done by Schiffino and Merril (Schiffino and Merril, 1993) in the temperature range of 230-350 °C using ideal gas heat capacities and the following expression was obtained (*T* in K):

Table 4
Summary of the published rate equations

Reference	The rate equation	
Padmanabhan, 1972	$-r_M = \frac{2r_0 P_M^{1/2}}{P_M^{1/2}+bP_W}$	(10)
Klusacek and Schneider, 1982	$-r_M = \frac{kK_M C_M}{\left(1+2\sqrt{K_M C_M}+K_W C_W\right)^2}$	
	$-r_M = \frac{kK_M {C_M}^2}{\left(1+2\sqrt{K_M C_M}+K_W C_W\right)^3}$	(11)
	$-r_M = \frac{kK_M {C_M}^2}{\left(1+2\sqrt{K_M C_M}+K_W C_W\right)^4}$	
Bercic et al., 1992	$-r_M = \frac{k_s K_M{}^2\left({C_M}^2-C_W C_D/K\right)}{\left(1+2\sqrt{K_M C_M}+K_W C_W\right)^4}$	(12)
Mollavali et al., 2008	$-r_M = \frac{k_2 P_M-\left(k_2/K_{eq}\right)(P_D P_W/P_M)}{K_M P_M+(P_W/K_W)+1}$	(13)
Moradi et al., 2010	$-r_M = \frac{k_s K_M{}^2 C_M{}^2}{(1+K_M C_M+K_W C_W)^2}$	
	$-r_M = \frac{k_s K_M{}^2 C_M{}^2}{\left(1+2(K_M C_M)^{2/3}+K_W C_W\right)^3}$	(14)
	$-r_M = \frac{k_s K_M{}^2 C_M{}^2}{(1+2(K_M C_M)^2+K_W C_W)^4}$	
Zhang et al., 2011	$-r_M = \frac{kP_M\left(1-P_W P_D/P_M^2\right)}{\left(1+\sqrt{K_M P_M}+K_W P_W\right)^2}$	(15)

$$\ln K = -1.7 + {}^{3220}/_{T} \quad (16)$$

Diep and Walnwright presented an extensive literature review on the equilibrium condition in the reaction and a more general temperature-dependence of *K*, is given elsewhere (Diep and Walnwright, 1987):

$$\ln K = {}^{2835.2}/_{T} - 1.675 \ln T - 2.39 * 10^{-4} - 0.21 * 10^{-6} T^2 - 13.36 \quad (17)$$

A new relation has also been presented by H. T. Zhang (H. T. Zhang et al. 2001):

$$\ln K = {}^{4019}/_{T} + 3.707 * \ln T - 2.783 * 10^{-3} T + 3.8 * 10^{-7} T^2 - 6.561 * {}^{10^4}/_{T^3} - 26.64 \quad (18)$$

2.3. Mesh study and processing description

The geometry of reactor with its boundary conditions as shown in Figure 2 is constructed in Gambit and a structured mesh is connected to it. The first important step in CFD simulations is to check the grid independency. The reaction is simulated in many grids with different cell sizes. After the solutions were converged, the change of various parameters (such as velocity, pressure, temperature, and methanol conversion) in different meshes was so small in a cell size less than 0.019 cm with an acceptable CPU time. Therefore, we chose the grid with this cell size for our investigations. The differential equations in the finite volume method were discretized. A steady axial-symmetry pressure-based solver with SIMPLE pressure-velocity coupling in FLUENT was employed. In Functions Hook menu, we hooked the reaction kinetic rate model via UDF.

In all cases, the numerical computations were considered to be converged when the scaled residuals of the different variables were lower than 10^{-5} for continuity, 10^{-11} for energy, and 10^{-6} for the other variables. Mass-flow-inlet and outflow boundary conditions were used for the reactor inlet and outlet respectively.

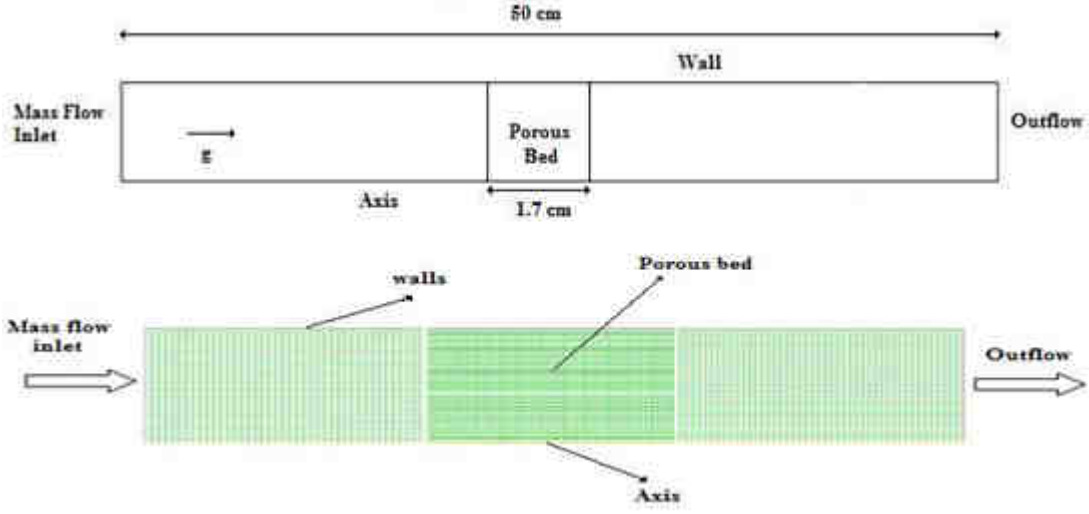

Figure 2
A schematic of reactor geometry and structured mesh

3. Results and discussion

3.1. Validation

The validation stage is presented in two sections of hydrodynamics and reaction validation. The reactor hydrodynamics is validated by pressure drop factor. The pressure drop from simulation results

is equal to 347.666 (KPa/m) and Ergun's equation prediction is 348.241 KPa/m, which results in a relative error of 0.164844%. Before continuing to the reaction validation, some explanations are required. Bercic supposed that the surface reaction with Langmuir-Hinshelwood concept was a controlling step and dissociative adsorption of methanol on the surface of γ-Al_2O_3 took place (Bercic and Levec, 1992). In detailed he supposed:

$$\begin{array}{ll} 2\times (CH_3OH + 2s \leftrightarrow CH_3s + OHs) & \text{(in equilibrium)} \\ 2CH_3s + 2OHs \leftrightarrow CH_3OCH_3s + H_2Os + 2s & \text{(surface reaction, rate controlling)} \\ H_2Os \leftrightarrow H_2O + s & \text{(in equilibrium)} \\ CH_3OCH_3s \leftrightarrow CH_3OCH_3 + s & \text{(in equilibrium)} \end{array} \quad (19)$$

With this mechanism and applying the method which has been further developed by Hougen (Hougen and Watson, 1943), one may have:

$$\hat{r} = k a_{CH3s}{}^2 a_{OHs}^2 - k' a_{CH_3OCH_3s} a_{H2Os} a_{vs}^2 \quad (20)$$

$$L = a_{vs} + 2a_{CH3s} + a_{H2OS} + a_{CH_3OCH_3s} \quad (21)$$

$$\hat{r} = \frac{k.L^4 K^2_{MeOH} \left(C_{MeOH}{}^2 - {}^{C_{DME}C_{H2O}}/_{K}\right)}{\left(1+2\sqrt{K_{MeOH}C_{MeOH}}+K_{H2O}C_{H2O}\right)^4} \quad (22)$$

The adsorption term for DME was neglected since the DME adsorption constant was too small compared to the adsorption constants of methanol and water (Bercic and Levec, 1992). $\hat{r}, k, \text{and } k'$ represent the rate of the reaction, forward, and backward reaction coefficients respectively. a_i is the concentration of spice *i* on catalyst surface; a_{vs} and L stand for the concentrations of vacant adsorption sites and the total active site of the catalyst respectively. K is also the equilibrium constant of overall reaction; K_i represents the adsorption constant of component *i*. Also, C_i is the concentration of component *i* in main fluid phase. With the comparison of Equation 12 and 22, one may obtain:

$$k_s = kL^4 \quad (23)$$

This means that at least the k_s in Equation 12 is catalyst-type dependent. The original relations for temperature-dependent parameters in Equation 12 are:

$$\begin{aligned} k_s &= 5.35 * 10^{13} \exp\left({}^{-17280}/_{T}\right) \\ K_M &= 5.39 * 10^{-4} \exp\left({}^{8487}/_{T}\right) \\ K_W &= 8.47 * 10^{-2} exp\left({}^{5070}/_{T}\right) \end{aligned} \quad (24)$$

k_s is a kinetic parameter and the other parameters in Bercic rate equation are the adsorption equilibrium constants of different species. According to Equation 23, it is needed to determine a relation in terms of temperature for k_s which is suitable for the specified catalyst. In this regard, a one-dimensional homogenous model of the reactor based on Ahmadi Marvast's study (Ahmadi Marvast et al., 2005) is derived and solved by finite deference method using MATLAB codes. By means of the genetic algorithm (GA) toolbox of MATLAB, at any inlet temperature, the best k_s value is determined in order to achieve a methanol conversion as close to experimental data as possible. After that the best Arrhenius and Van't Hoff type relation for k_s with respect to temperature is derived:

$$k_s = 2.523 \times 10^{10} * \text{EXP}(-11877.23/T) \quad (25)$$

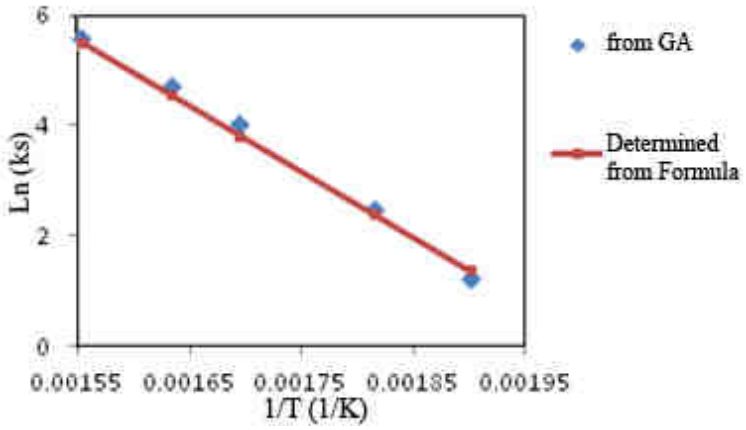

Figure 3
k_s determined from GA toolbox and Equation 25

The results obtained from GA toolbox and the results of the Equation 25 are summarized in Figure 3. The mean relative error of k_s determined from Equation 25 with respect to the GA results is equal to 3.2%. Via this modified Bercic rate and with the two-dimensional homogenous model, the simulation results from FLUENT have been validated by experimental data and the results are shown in Figure 4. The mean relative prediction error is about 14% and it is 38% less than the error of simulation results with original Bercic rate equation.

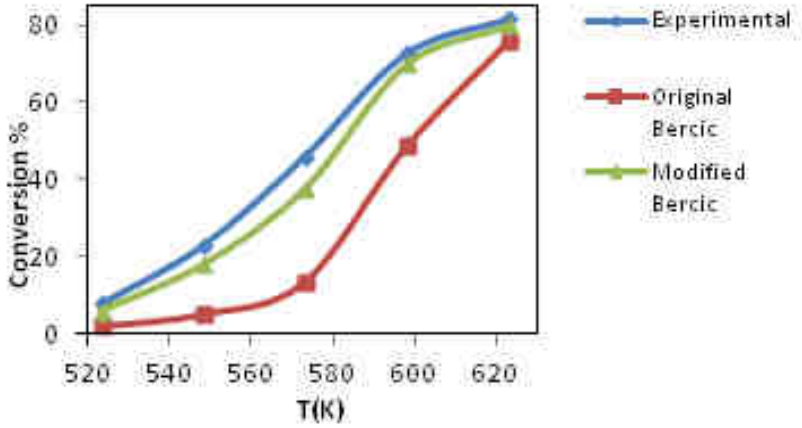

Figure 4
Simulation and experimental methanol conversion

In according to some works (Schiffino and Merril, 1993; Zuo et al., 2011), two mechanisms are simultaneously possible for DME production in methanol dehydration. Schiffino especially claimed that the two methanol molecules dissociation mechanism was dominated above 563 K and the other mechanism was more observed at temperatures lower than this. Bercic rate equation was derived in a temperature range of 563-633 K. Bercic considered the two methanol molecules dissociation mechanism and forgot about the other mechanisms. The distance depicted in Figure 4 about 563 K is related to this assumption. Additionally, the Bercic rate equation has an adequate performance for high temperatures as shown in Figure 4.

3.2. Methanol conversion variation

According to Le Chatelier's principle in an equimolecular reaction and Figure 5, the pressure does not affect the conversion of methanol and hence the key operating parameters in the reaction are temperature and space velocity. The effects of temperature and WHSV are investigated on the conversion of methanol for WHSV= 10 to 150 h^{-1} and T_{inlet}=523 to 623 K.

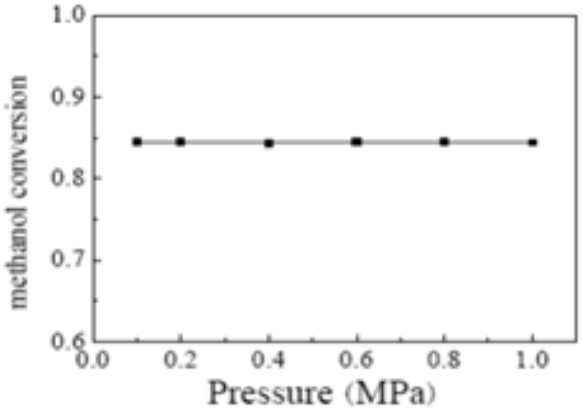

Figure 5
Effect of pressure on methanol conversion (Zhang et al., 2011)

The results are shown in Figure 6. In according to this figure, at WHSV equal to 10 h^{-1} and at a temperature of 563.15 K, the maximum conversion of 85.03% is obtained. It means that the best condition took place at a minimum value of WHSV at intermediate temperatures. In Figure 6, it is obvious that the effect of temperature on the conversion of methanol is much greater than that of WHSV.

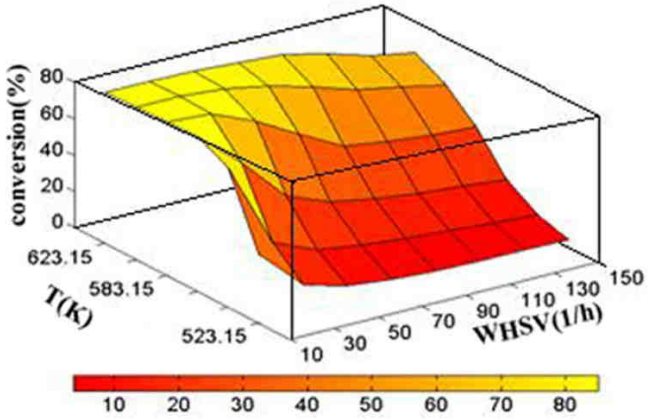

Figure 6
Conversion of methanol (%) versus inlet temperature and WHSV

For correlation (R^2) values smaller than 0.9755, the surface fitting toolbox of MATLAB was used for the prediction of methanol conversion. The results from this toolbox are shown in Figure 7:

$$X(\%) = 43.29 + 38.04\,T_{Nor} - 17.44W_{Nor} - 2.439\,T_{Nor}^2 + 0.7644\,T_{Nor}W_{Nor} + 5.739W_{Nor}^2 - 5.303T_{Nor}^3 + 5.095T_{Nor}^2W_{Nor} - 4.002T_{Nor}W_{Nor}^2 + 0.9731T_{Nor}^4 - 0.2555T_{Nor}^3W_{Nor} - 2.255T_{Nor}^2W_{Nor}^2 \quad (26)$$

where, T_{Nor} =T_{inlet}/573.2 and W_{Nor} = WHSV/80.

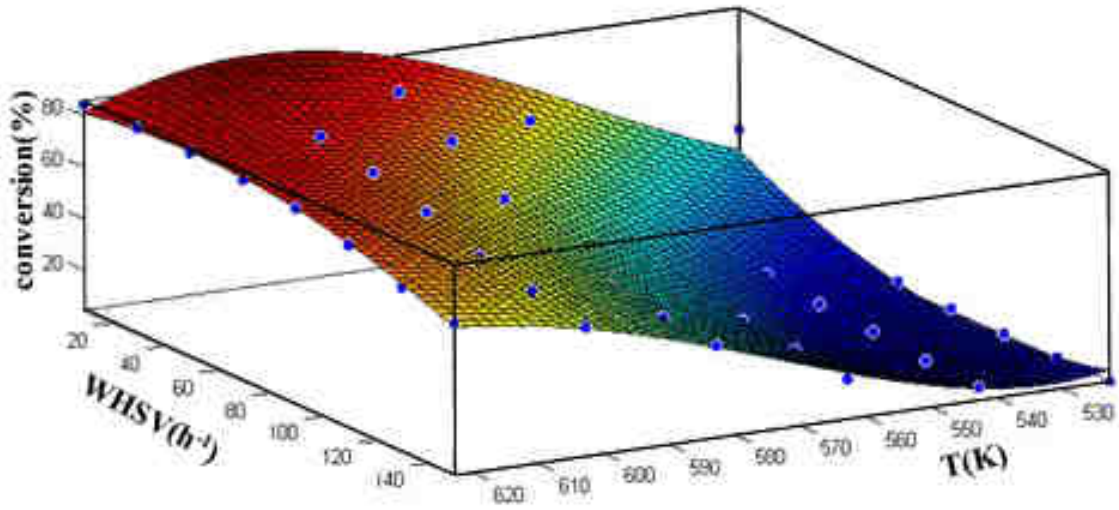

Figure 7
Results from surface fitting toolbox of MATLAB; comparison between the calculated conversions of methanol using the proposed equation (Surface) and the simulation results (Points).

The profile of velocity and concentration at WHSV=10 h^{-1} and T=563.15 K is shown to better understand the reactor conditions. In Figure 8, the contours of the velocity and the centerline velocity along the reactor are presented. Due to the increase of temperature and accordingly the decrease of density along the reactor bed, the minimum velocity magnitude is about 0.063 m/s, which is detected at the inlet, and the maximum velocity is at the outlet (about 0.13 m/s), which is about twice the inlet value. Also, the temperature-dependent properties of mixture varied along the reactor and C_{Pf} was varied within 2001.92 to 2998.89 j/kg.K; viscosity and thermal conductivity were between 1.85e-05 to 1.97e-05 kg/m.s and 0.02 to 0.047 w/m.K respectively. The mass fraction of all materials in reaction is shown in Figure 9 and Figure 10; it is seen from these figures that the most mass fraction variation is occurred at 41% of total bed length. The ultimate methanol conversion is about 85.03%.

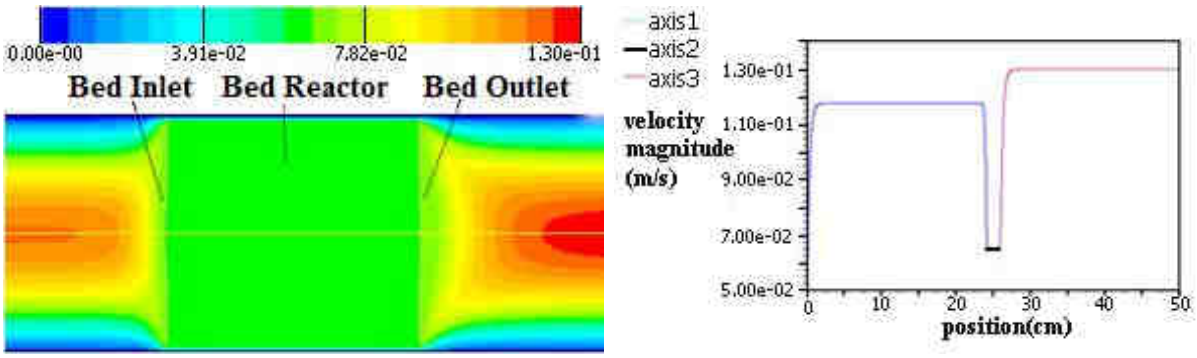

Figure 8
Velocity contours and velocity of centerline along of reactor bed

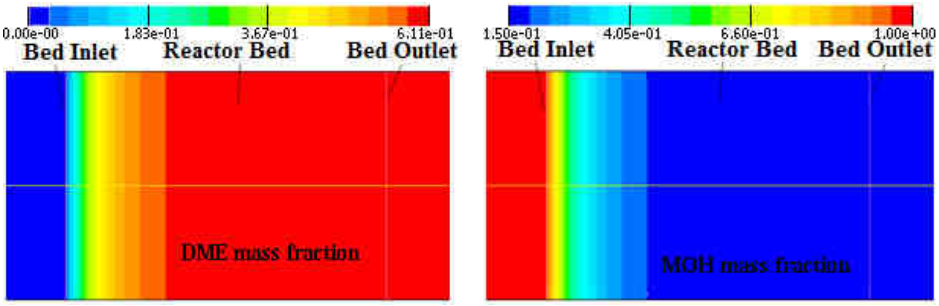

Figure 9
Mass fraction contours of CH_3OCH_3 and CH_3OH

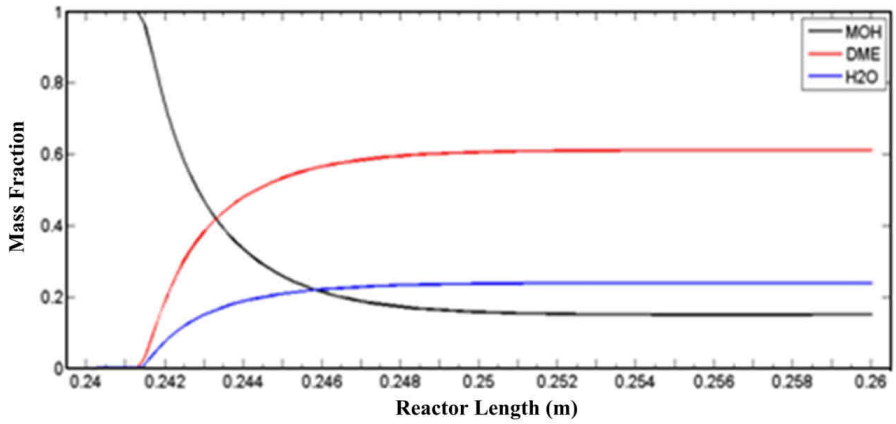

Figure 10
Mass fraction of all materials in reaction vs reactor bed length

3.3. Effect of inlet temperature on conversion

The effect of inlet temperature on methanol conversion in the range of 523.15-623.15 K at different WHSV's is shown in Figure 11. As presented in this figure, the conversion of methanol rises by increasing temperature except at WHSV values equal to 10 and 30 h^{-1} at which methanol conversions get the equilibrium conversions due to the low velocity of the reactants. Because the equilibrium conversion of an exothermic reaction decreases when temperature rises, the conversions at WHSV equal to 10 and 30 h^{-1} also drop.

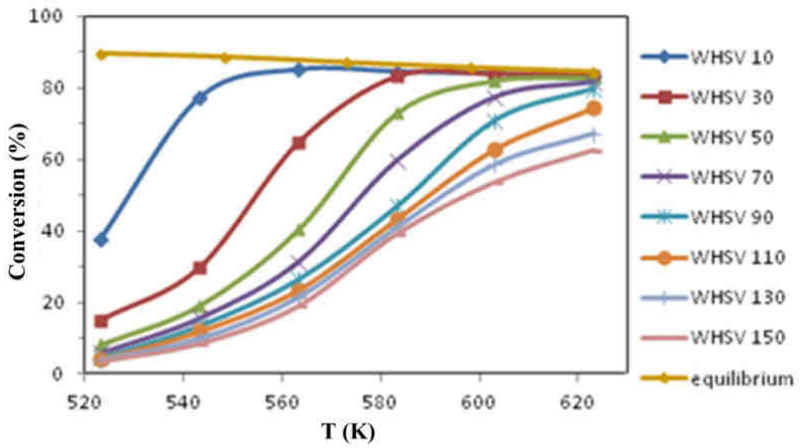

Figure 11
Conversion of reaction (%) at different temperatures with the modified Bercic rate equation

3.4. Effect of WHSV on methanol conversion

The effect of WHSV on methanol conversion in the range of 10-150 h^{-1} at different inlet temperatures is also depicted in Figure 12. As can be seen, by increasing WHSV the velocity of the reactant rises while the residence time decreases; therefore, the conversion surely decreases. At a temperature of 623.15 K, the conversion of reaction is a weak function of WHSV.

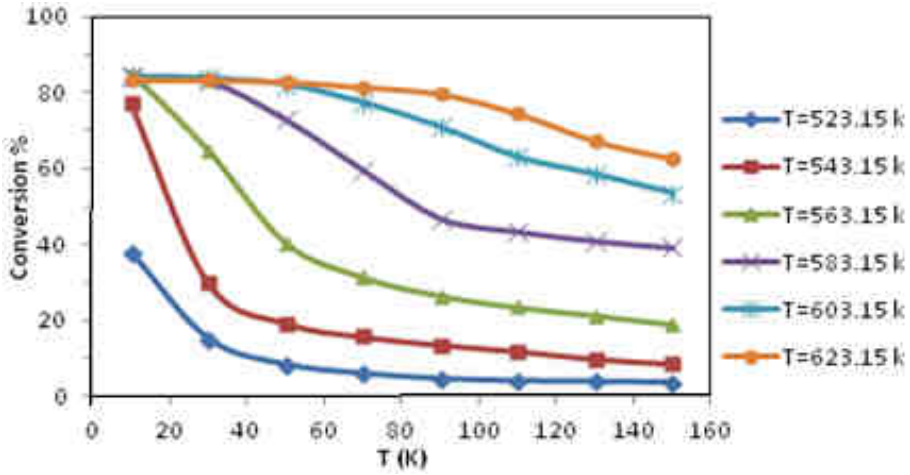

Figure 12
Conversion of reaction (%) versus WHSV with the modified Bercic rate equation

3.5. Inlet water content effect on methanol conversion

The effect of inlet water content on reaction is also studied. This effect is investigated in two levels of water mass fractions, namely0.05 and 0.1, in inlet feed in the temperature range of 523.15-623.15 K and in the WHSV range of 50-130 h^{-1}. The summarized results are shown in Figure 13. The presence of water in the reactor inlet has a negative effect on methanol conversion because water is a product of the reaction and according to Le Chatelier's principle the rate of direct reaction under this condition decreases. For finding a quantitative relation to determine the effect of inlet water mass fraction on methanol conversion, we used the surface fitting toolbox of MATLAB. The below relation with an R^2 value of 0.9940 is obtained:

$$\begin{aligned} X(\%) = {} & 18.97 + 41.35T_{Nor} + 11.3W_{mNor} + 12.38T_{Nor}^2 - 9.151T_{Nor}W_{mNor} + 16.9W_{mNor}^2 \\ & - 8.061T_{Nor}^3 + 3.099T_{Nor}^2W_{mNor} - 1.08T_{Nor}W_{mNor}^2 - 22.47W_{mNor}^3 \\ & - 5.243T_{Nor}^4 + 2.494T_{Nor}^3W_{mNor} + 0.06021T_{Nor}^2W_{mNor}^2 + 2.174T_{Nor}W_{mNor}^3 \end{aligned} \quad (27)$$

where, $T_{Nor} = {}^{T(K)}/_{573.1}$, $W_{mNor} = (1 + Wa)\frac{W(h^{-1})}{35.96}$, and Wa is the mass fraction of water.

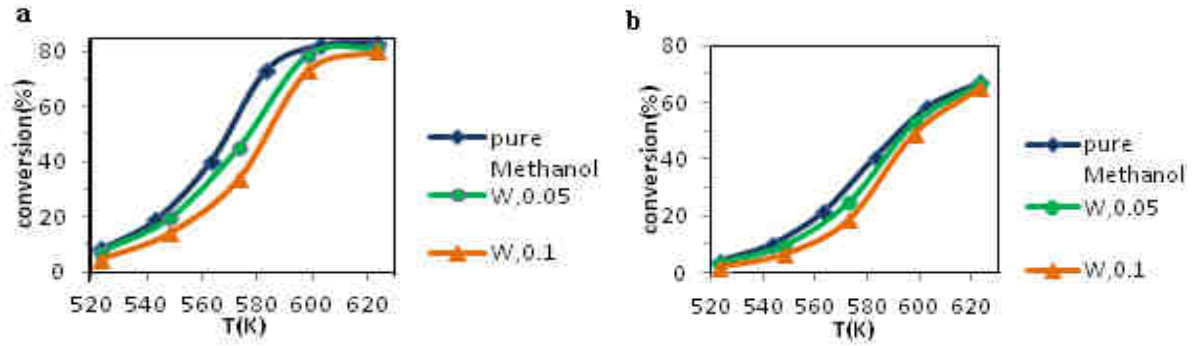

Figure 13
Methanol conversion versus water mass fraction at (a) WHSV=50 h^{-1}; (b) WHSV= 130 h^{-1}.

4. Conclusions

A two-dimensional homogenous model constructed in FLUENT 6.3.26 is validated by the experimental data. The model predicts the pressure drop within an error of 0.16% relative to Ergun equation. From all rate equations listed in Table 4, the Bercic model has the best prediction of methanol conversion. Using the modified Bercic rate equation in the simulation causes the model to predict methanol conversion with an average error of 14%. This shows an improvement of about 38% in the simulation results by applying the original Bercic rate equation. The simulations were carried out in a temperature range of about 250 °C to 350 °C in a wide space velocity range of 10 to 150 $gr.hr^{-1}/gr_{cat}$. The maximum conversion of reaction was obtained in a temperature range of 563.15 to 623.15 K and at a WHSV value of 10 hr^{-1} with a methanol conversion of 83~85%;the best condition is obtained at WHSV=10 h^{-1}, T=563.15 K, and conversion=85.03%. Two correlations are presented for obtaining the conversion of methanol in two situations, namely pure methanol and the presence of water in the inlet feed; the negative effect of water as a reactant is formulated. The allowable operating range was obtained at temperatures of 290~350 °C and at space velocities of 10~90 $gr.hr^{-1}/gr_{cat}$. Under these conditions, the obtained methanol conversion is about 75~85%. The results of the study indicate that the feed temperature is the major factor controlling the concentration and temperature profiles (and also the conversion). At temperatures higher than 583.15 K, the slight effect of space velocity on the methanol conversion is observed. It is concluded that the negative effect of increasing the space velocities can be compensated for by increasing temperature.

Nomenclature

a_i	: Concentration of i-component on catalyst surface
a_{vs}	: Concentrations of vacant adsorption sites (equivalent moles/unit mass of catalyst)
C_j	: Concentration of j-component in bulk fluid ($kmol/m^3$)
c_{pf}	: Specific heat capacity of fluid (kJ/kg.K)
D_{ejm}	: Effective diffusivity of j-species (m^2/s)
D_{jm}	: Diffusivity of j-species in mixture (m^2/s)
D_{jk}	: Binary diffusivity of j- in k- species (m^2/s)
d_p	: Particle diameter (m)
d_t	: Diameter of reactor (m)
$F_{i=z,r}$	: Extra terms in the momentum balance equation
ΔH	: Heat of reaction (kJ/kmol)
K	: Equilibrium constant of overall reaction
k,k'	: Forward and reverse reaction velocity constants
k_i	: Adsorption constant of component *i* ($m^3/kmol$)
k_s	: Rate constant of surface reaction (kmol/kgcat.s)
L	: Total molal adsorption sites/unit mass of catalyst
M	: Molecular weight (kg/kmol)
R	: Universal gas constant
$\hat{r}_i$	: Rate of ith reaction (kmol/kgcat.s)
WHSV	: Weight hourly space velocity (h^{-1})
Greek Symbol	
ε	: Porosity of solid catalyst
ϕ	: Particle sphericity factor
ℓ	: Mean free path of the gas molecule (m)
λ_{er}	: Redial effective conductivity of mixture (kJ/m.K.s)
μ	: Viscosity (kg/m.s)

ρ_b	: Bulk density of bed (kg/m^3)
ρ	: Mixture density (kg/m^3)
τ_o	: Tortuosity of catalyst particle

References

Ahmadi Marvast, M., Sohrabi, M., Zarrinpashne, S., Baghmisheh, G., Fischer-Tropsch Synthesis: Modeling and Performance Study for Fe-HZSM5 Bifunctional Catalyst, Chemical Engineering Technology, Vol. 28, p.78-86, 2005.

Andrews, A. T., Dixon, A. G., Fan, L. S., Fox, R. O., Ge, Y., Kuipers, J.A.M., Nijemeisland, M., Stitt, E.H., Sundaresan, S., Van Den Akker, H.E.A., et al., Advances in Chemical Engineering, Elsevier Inc. Publications, Vol. 31, p. 395, 2006.

Andrigo, P., Bagatin, R. and Pagani, G., Fixed Bed Reactors, Catalysis Today, Vol. 52, p. 197-221, 1999.

Bercic, G. and Levec, J., Catalytic Dehydration of Methanol to Dimethyl Ether, Kinetic Investigation and Reactor Simulation, Ind. Eng. Chem. Res., Vol. 32, p. 2478-2484, 1993.

Bercic, G. and Levec, J., Intrinsic and Global Reaction Rate of Methanol Dehydration Over γ-Al_2O_3 Pellets, Ind. Eng. Chem. Res., Vol. 31, p.1035-1040, 1992.

Brokaw, R. S., Predicting Transport Properties of Dilute Gases. I and EC Process Design and Development, Vol. 8, p.240-253, 1969.

Cheung, P., Bhan, A., Sunley, G. J., Iglesia, E., Selectivity Carbonylation of Dimethyl Ether to Methyl Acetate Catalyzed by Acidic Zeolites, Angew. Chem. Int., Vol. 45, p. 1617-1620, 2006.

Diep, B. T. and Walnwright, M. S., Thermodynamic Equilibrium Constants for the Methanol-dimethyl Ether-water System, J. Chem. Eng. Data, Vol. 32, p. 330-333,1987.

Dixon, Anthony, G., Correlations for Wall and Particle Shape Effects on Fixed Bed Bulk Voidage, The Can. J. Chem. Eng., Vol. 66, p. 705-708,1988.

Dybbs, A., Edwards, R. V., Bear, J., Fundamentals of Transport Phenomena in Porous Media, Martinus Nijhoff, Dordrecht, 1003 p, 1984.

Ergun, S., Fluid Flow Through Packed Columns, Chemical Engineering Progress, Vol. 48, p. 89-94,1952.

Farsi, M., Jahanmiri, A. and Eslamloueyan, R., Modeling and Optimization of MeOH to DME in Isothermal Fixed-bed Reactor, International Journal of Chemical Reactor Engineering, Vol. 8, P. A79, 2010.

Fazlollahnejad, M., Taghizadeh, M., Eliassi, A., Bakeri, G., Experimental Study and Modeling of an Adiabatic Fixed-bed Reactor for Methanol Dehydration to Dimethyl Ether, Chinese Journal of Chemical Engineering, Vol. 17, p. 630-634, 2009.

Freund, H., Zeiser, T., Huber, F., Klemm, E., Brenner, G., Durst, F., Emig, G., Numerical Simulations of Single Phase Reacting Flows in Randomly Packed Fixed-bed Reactors and Experimental Validation, Chemical Engineering Science, Vol. 58, p. 903-910, 2003.

Ghavipour, M., MS, Reaction Rate Investigation by Experimental Study and Fixed-bed Reactor Modeling for Methanol to DME Reaction Over γ-Al_2O_3, MS Thesis, Petroleum University of Technology, Ahwaz, 86 p, 2011.

Hosseini, S. Y., Khosravi Nikou, M. R., Synthesis and Characterization of Different γ-Al_2O_3 Nanocatalysts for Methanol Dehydration to Dimethyl Ether, Vol. 10, P. A65,2012.

Hougen, O. A. and Watson, K. M., Solid Catalysts and Reaction Rates: General Principles, Industrial and Engineering Chemistry, Vol. 35, p. 529-541, 1943.

Ivanova, S., Vanhaecke, E., Dreibine, L., Louis, B., Pham, C., Pham-Huu, C., Binderless HZSM-5

Coating on b-SiC for Different Alcohols, Applied Catalysis, Vol. 359, p. 151-157,2009.

Khom-in, J., Praserthdam, P., Panpranot, J., Mekasuwandumrong, O., Dehydration of Methanol to Dimethyl Ether over Nanocrystalline Al2O3 with Mixed γ- and χ-crystalline Phases, Catalysis Communications, Vol. 9, p. 1955-1958, 2008.

Klusacek, K. and Schneider, P., Multicomponent Diffusion of Gases in a Model Porous Catalyst During Methanol Dehyration, Chemical Engineering Science, Vol. 36, p. 517-522, 1981.

Lanfrey, P., Kuzeljevic, Z. V. and Dudukovic, M. P., Tortuosity Model for Fixed Beds Randomly Packed with Identical Particles, Chemical Engineering Science, Vol. 65, p. 1891-1896, 2010.

Lu, W.-zhi, Teng, L.-hua and Xiao, W.-de, Simulation and Experiment Study of Dimethyl Ether Synthesis from Syngas in a Fluidized-bed Reactor, Chemical Engineering Science, Vol. 59, p. 5455-5464, 2004.

Mollavali, M., Yaripour, F., Atashi, H., Sahebdelfar, S., Intrinsic Kinetics Study of Dimethyl Ether Synthesis from Methanol on γ-Al_2 O_3 Catalysts, Ind. Eng. Chem. Res., Vol. 47, p. 3265-3273, 2008.

Moradi, G., Yaripour, F., Abbasian, H., Rahmanzadeh, M., Intrinsic Reaction Rate and the Effects of Operating Conditions in Dimethyl Ether Synthesis from Methanol Dehydration, Korean J. Chem. Eng., Vol. 27, p. 1435-1440, 2010.

Olah, G. A., Goeppert, A. and Prakash, G. K. S., Beyond Oil and Gas: The Methanol Economy, Wiley-VCH Co. KGaA Publication, 334 p., 2009.

Padmanabhan, V. R. and Eastburn, F. J., Mechanism of Ether Formation from Alcohols over Alumina Catalyst, Journal of Catalysis, Vol. 24, p. 88-91, 1972.

Raoof, F., Taghizadeh, M., Eliassi, A., Yaripour, F., Effects of Temperature and Feed Composition on Catalytic Dehydration of Methanol to Dimethyl Ether over γ-alumina, Fuel, Vol. 87, p. 2967-2971, 2008.

Schiffino, R. S. and Merril, R. P., A Mechanistic Study of the Methanol Dehydration Reaction on y-Alumina Catalyst, J. Phys. Chem., Vol. 97, p. 6425-6435, 1993.

Schuurman, Y., Aspects of Kinetic Modeling of Fixed Bed Reactors, Catalysis Today, Vol. 138, p. 15-20, 2008.

Semelsberger, T. A., Borup, R. L. and Greene, H. L., Dimethyl Ether (DME) as an Alternative Fuel, Journal of Power Source, Vol. 156, p. 497-511, 2006.

Shahhosseini, S., Alinia, S. and Irani, M., CFD Simulation of Fixed Bed Reactor in Fischer-tropsch Synthesis of GTL Technology, World Academy of Science, Engineering and Technology, Vol. 60, p. 585-589, 2009.

Spivey, J. J., Review: Dehydration Catalysts for the Metanol/Dimethyl Ether Reaction, Chemical Engineering Communications, Vol. 110, p. 123-142, 1991.

Tilton, J. N. and Hottel, H. C., Perry's Chemical Engineering's Handbook 8th Ed., McGraw-Hill Publication, 2008.

Yoon, E. S. and Han, C., A Review of Sustainable Energy-Recent Development and Future Prospects of Dimethyl Ether (DME), Computer Aided Chemical Engineering, Vol. 27, p. 169-175, 2009.

Zhang, H. T., Cao, F. H., Liu, D. H., Fang, D. Y., Thermodynamic Analysis for Synthesis of Dimethyl Ether and Methanol from Synthesis Gas, Journal of ECUST, Vol. 27, p. 198-201, 2001.

Zhang, L., Zhang, H. T., Ying, W. Y., Fang, D. Y., Intrinsic Kinetics of Methanol Dehydration over Al_2O_3 Catalyst, Engineering and Technology, Vol. 59, p. 1538-1543, 2011.

Zuo, Z., Huang, W., Han, P., Gao, Z., Li, Z., Theoretical Studies on the Reaction Mechanisms of AlOOH- and γ-Al_2O_3 -catalysed Methanol Dehydration in the Gas and Liquid Phases, Applied Catalysis A, General, Vol. 408, p. 130-136, 2011.